JOURNAL OF GEOPHYSICAL RESEARCH, VOL. 103, NO. A6, PAGES 12,023–12,035, JUNE 1, 1998

Very low frequency waves in the heliosphere: Ulysses observations

Naiguo Lin,[1] P. J. Kellogg,[1] R. J. MacDowall,[2] E. E. Scime,[3]
A. Balogh,[4] R. J. Forsyth,[4] D. J. McComas,[5] and J. L. Phillips[5]

Abstract. An overall profile of plasma wave activity in a frequency range of 0.2 to 448 Hz in the solar wind is presented using 6 years of Ulysses data which cover a large range of heliographic latitudes (0° to ±80°) at distances from 1 to 5 AU from the Sun. The spacecraft has continuously observed wave activity with peak power below the local electron cyclotron frequency f_{ce}. Four distinct types of fluctuation phenomena have been observed: (1) enhanced electromagnetic fluctuations associated with the interplanetary shocks and heliospheric current sheet crossings and other solar wind turbulence; (2) enhanced electromagnetic fluctuations associated with compression regions of high-speed stream interfaces, which were observed in periods of increasing solar wind velocity; (3) electric fluctuations associated with the expanding solar wind, which were observed in periods of decreasing solar wind velocity; and (4) enhanced electric fluctuations in the high-latitude fast solar wind plasma. The fourth type of wave activity was observed nearly continuously with the relative power observed peaked near the local f_{ce}. The first three types of waves were observed in the heliomagnetic streamer belt flows, where the spacecraft frequently encountered enhanced solar wind turbulence, interplanetary shocks, and current sheet crossings. The electromagnetic wave bursts (types 1 and 2) are likely to be whistler mode. The occurrences of apparently electrostatic waves during periods of expanding solar wind are coincident with significant reductions in the electron heat flux intensity. The generation mechanism of these electrostatic waves is still under investigation, but the observations may imply that these waves reduce the intensity of the heat flux through enhanced wave particle scattering associated with a heat flux instability.

1. Introduction

Prior to the Ulysses mission, very low frequency (VLF) plasma waves in the solar wind have been observed and studied, mostly based on data obtained within 1 AU from the Sun and near the ecliptic plane (see, for example, review papers by *Gurnett* [1991] and *Schwartz* [1980], and references therein). Electromagnetic noise with frequency between the ion (f_{ci}) and electron (f_{ce}) cyclotron frequencies has been observed in the solar wind in earlier missions. It is commonly believed that these waves are whistler mode emissions, as their frequency range suggested. Helios 1 and 2 have observed whistler mode fluctuations at all radial distances between 0.31 and 0.86 AU using search coils which cover a frequency range from about 4 Hz to 2.2 kHz [*Neubauer et al.*, 1977a, b; *Beinroth and Neubauer*, 1981]. They also found that the whistler wave intensity tended to increase with decreasing radial distance from the Sun.

Whistler waves associated with solar wind turbulence, for example, waves near interplanetary shocks, have drawn much attention and have been studied intensively. Observations from Helios 1 [*Neubauer et al.*, 1977a, b] and Helios 2 [*Gurnett et al.*, 1979a] and from ISEE 3 [*Kennel et al.*, 1982; *Coroniti et al.*, 1982] have shown that magnetic noise in the above mentioned frequency range was strongly enhanced by interplanetary shocks, and the enhancement extended many hours downstream of the shocks. In a study of several shock events, *Coroniti et al.* [1982] suggested that the whistler waves they observed were generated propagating at large angles to the ambient magnetic field based on analysis of B/E ratio. Helios observations found [*Beinroth and Neubauer*, 1981] that magnetic wave power intensifies in the vicinity of stream inter-

[1]School of Physics and Astronomy, University of Minnesota, Minneapolis.
[2]NASA Goddard Space Flight Center, Greenbelt, Maryland.
[3]Physics Department, West Virginia University, Morgantown.
[4]Imperial College of Science and Technology, London.
[5]Los Alamos National Laboratory, Los Alamos, New Mexico.

Paper number 98JA00764.
0148-0227/98/98JA-00764$09.00

faces and decreases with decreasing velocity, often interrupted by sharp and brief enhancements or by the next fast stream. They suggested that the waves were generated locally.

Several free-energy sources for the whistler mode instabilities in the solar wind have been suggested. Among them, the electron heat flux has been suggested as a possible free energy for instabilities in the solar wind. These instabilities include fast magnetosonic waves, Alfven waves, and whistler mode waves [*Gary et al.*, 1975a, b], ion acoustic waves [*Gurnett et al.*, 1979b], lower hybrid waves [*Marsch and Chang*, 1982, 1983], and others. *Neubauer et al.* [1977b] suggested that the field-aligned current might drive the whistler mode instability. *Scarf et al.* [1967] suggested that whistler waves could be produced by ions with parallel velocity larger than the wave phase velocity, which interacted with the wave and excited an anomalous cyclotron resonance.

The unique orbit of Ulysses extends our observations into the solar polar regions and also to farther distances from the Sun for measurements of magnetic waves. Also, the Ulysses plasma wave instrument is unique for measuring low-frequency waves because the spin axis of the spacecraft is always nearly toward the Sun, and thus there is less photoelectron effect; and the measurements are extended to frequencies as low as fractions of hertzs. These advantages have been utilized to make a number of important observations of VLF plasma waves in the solar wind. In this study we report Ulysses observations of VLF wave activity in the solar wind during 1990-1996, as Ulysses completed its first solar polar orbit and started the second orbit. The observations cover a radial distance ranging from 1 to 5.5 AU and heliographic latitudes up to ±80°.

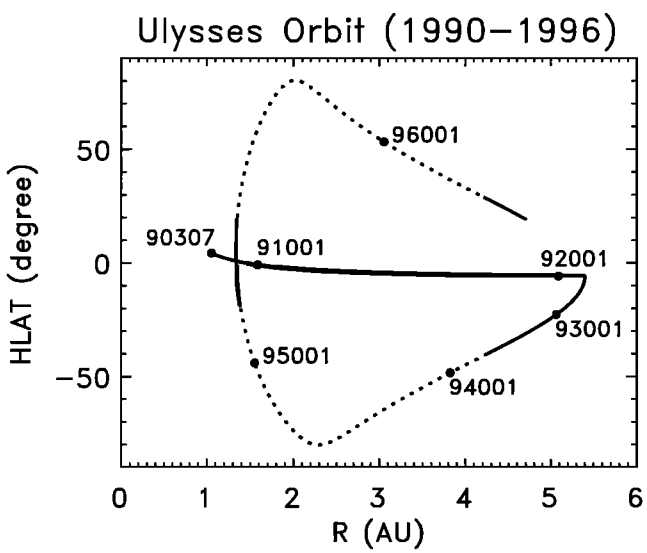

Figure 1. Ulysses orbit from 1990 to 1996, plotted in terms of the radial distance from the Sun and the heliographic latitude. The solid part of the trajectory is for the locations of Ulysses when it was within the heliospheric current sheet region, and the dotted part is for the locations in high-latitude fast solar wind.

Figure 1 shows the Ulysses orbit from 1990 to 1996, plotted in terms of the radial distance from the Sun and the heliographic latitude. The solid lines in the figure indicate the location of Ulysses in the region where the spacecraft regularly crossed the heliospheric current sheet and frequently encountered interplanetary shocks and other solar wind turbulence. This is the region of heliomagnetic streamer belt flows [*Bame et al.*, 1993], which encircle the heliomagnetic equator and extend outward, surrounding the embedded heliospheric current sheet. In this paper, we will refer to this region as the heliomagnetic streamer belt (HSB). The dotted lines indicate Ulysses locations when it was outside the HSB, in the fast solar wind stream (700-800 km/s). As indicated by the latitude-longitude maps of velocity [*Coles*, 1995], years of solar minimum are characterized by high-speed flow everywhere except in a low-velocity trough over the equatorial streamer belt that occupies a latitude range of $\sim \pm 20°$. We will see later that the characteristics of waves occurring inside and outside the HSB are very different.

In the following sections, we will first describe the data we used and the problems concerning background noise determination and then present the observations of plasma waves at frequencies between 0.2 and 448 Hz. This will be followed by discussions of the interpretation of the observed phenomena by comparing the new observations with the previous observations.

2. Instrumentation and Data

The low-frequency plasma wave data used in this study are obtained by the waveform analyzer (WFA) which is part of the unified radio and plasma wave (URAP) instrument [*Stone et al.*, 1992; *Kellogg et al.*, 1992] aboard the Ulysses spacecraft. The URAP experiment analyzes the signals on four antennas: one electric and one magnetic antenna aligned along the spin axis, which is always directed toward the Earth, and one electric antenna and one magnetic antenna perpendicular to the spin axis. The spin plane electric antenna consists of two monopoles of length 35.2 m each; with a spacecraft diameter of 2.6 m, this gives a tip-to-tip length of 73 m. The WFA provides spectral analysis of electric and magnetic signals in 10 low-band and 12 high-band channels, which cover a frequency range between 0.22 and 448 Hz. The data used are measurements made in the spacecraft spin plane with a 64-s time resolution. The measurements on the antenna aligned with the spin axis are not used here because of the higher noise level. The solar wind data (solar wind velocity, plasma density, and temperature) are obtained by the solar wind observations over the poles of the Sun (SWOOPS) experiment [*Bame et al.*, 1992]. The magnetic field data are obtained by the Ulysses magnetometer experiment [*Balogh et al.*, 1992]. The timing of shock encounters, which are identified on the basis of the magnetic and plasma observations jointly, is provided by the magnetometer team [*Balogh et al.*, 1995a; *Forsyth et al.*, 1996].

It is found that the background electric noise of the 10 low-band channels of the WFA data (from 0.22 Hz to 5.3

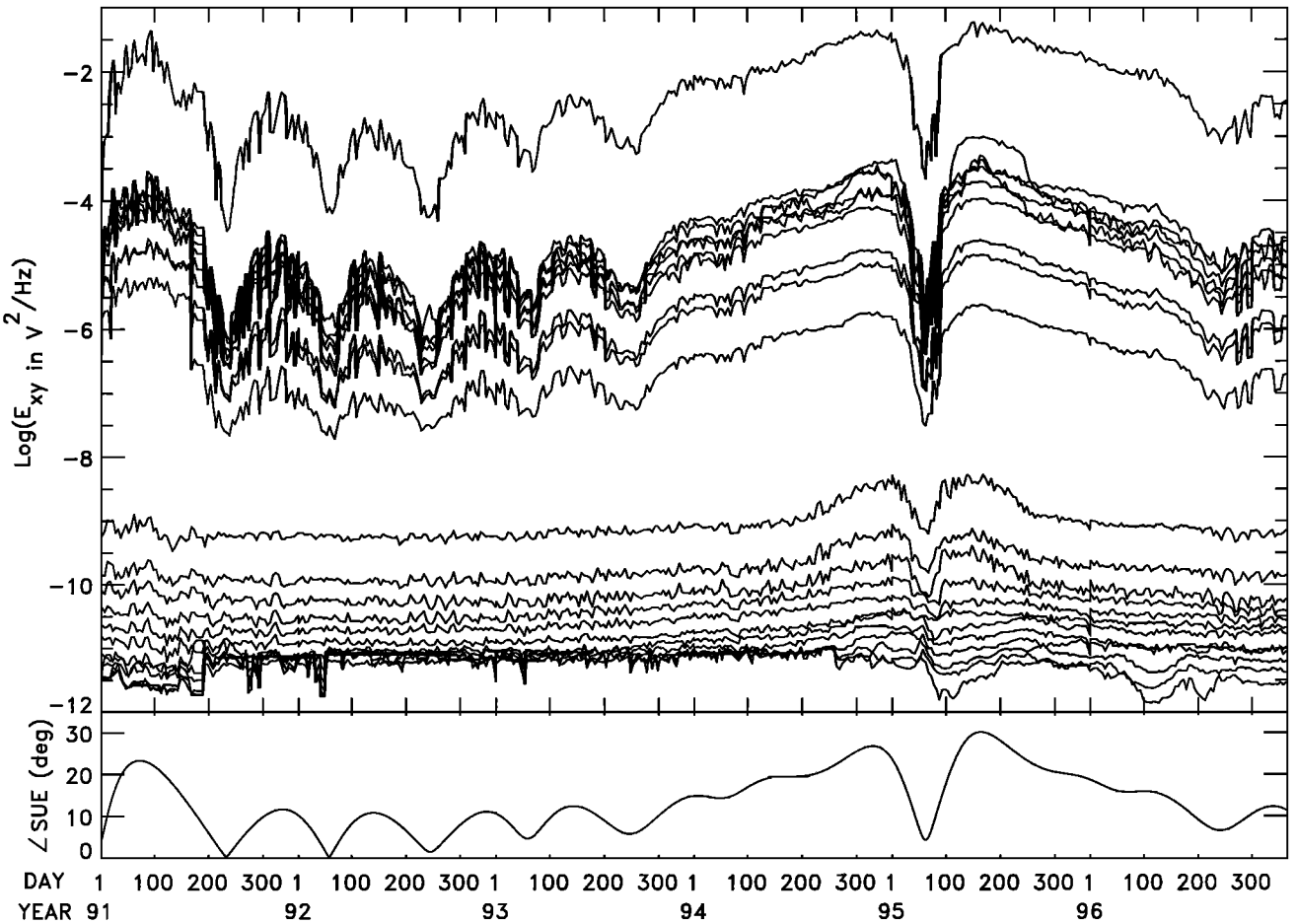

Figure 2. The background noise of 10 low-band and 12 high-band waveform analyser channels (at 1024 bit rate and when the plasma frequency receiver was in the fast scan mode) derived from the data for the years 1991-1996. The curves below 10^{-8} V^2/Hz are the high-band background. The solar aspect angle is plotted in the bottom panel.

Hz) varies with the solar aspect angle, i.e., the angle between the Sun, Ulysses, and the Earth (the SUE angle). Since the frequency range of interest includes these low frequencies, the determination of the background noise of the instrument becomes very important. The variation of the background noise occurs probably because of the existence of a sunward directed photoelectron cloud around the spacecraft, which affects measurements at the receiver input. The effect of the photoelectron cloud is evident in the measurements of the dc electric field (not shown), which produce one peak voltage in a spin period. The detailed analyses and discussion of the effects are a task of future work. The above effect does not affect the high band of the instrument, which is isolated from the lower frequencies by a high-pass filter.

The background noise level of the WFA is calculated as follows: For each channel, a background value is derived from the data in every 5-day period as the average over the 10% of the data with minimum values. These background values for all 5-day periods are then interpolated to obtain a background value for each day. Since the background noise for each channel varies with different scan modes of another instrument, the plasma frequency receiver (PFR), and with different bit rates, the calculations of the background noise are conducted separately for fast and slow PFR scan modes and at two different bit rates (1024 and 512). In the upper panel of Figure 2 we show as an example the time variation of the background noise in 10 low-band channels and 12 high-band channels for the years 1991-1996, at 1024 bit rate and when the PFR was at fast scan mode. The variation of the solar aspect angle for the same period is shown in the lower panel, which displays a correlation with the low-band background variation. The background of the high-band channels (9.3-448 Hz) was nearly constant except for the period from mid-1994 to mid-1995, when the high-band background varied with the solar aspect angle.

3. Wave Observations

Throughout the interplanetary medium, Ulysses has continuously observed a variety of wave activities with peak power below and near the local electron cyclotron frequency f_{ce}. Plate 1 shows the dynamic spectra of the electric noise measured in the spin plane for the

years 1991, 1995, and 1996. In the spectra, the wave power is expressed by the relative intensity, which is the ratio of the measured signal minus the background noise, divided by the background noise. With such dynamic spectra, we are able to identify the frequencies at which the wave activity is most intense. We may miss the waves whose intensity is below the instrument noise, but the overall pattern of the wave activity, which is correlated to other independent measurements (e.g., the ambient magnetic field and thus the electron cyclotron frequency, solar wind velocity, and the electron heat flux), as will be shown later, seems to justify the removal of the background noise.

In the entire year of 1991 the spacecraft was in the heliomagnetic streamer belt flows near the ecliptic plane heading for Jupiter (see Figure 1). In early 1995, the spacecraft reentered the HSB from the southern solar polar region and was traversing the region from about day 30 to 100 (between $\sim 20°$ and $-20°$ heliographic latitudes). After that, the spacecraft traveled in the northern high-latitude heliosphere for the rest of 1995 and most of 1996, until about day 219 of 1996 ($\sim 30°$), when the spacecraft started to see corotating structures, indicating the spacecraft was in the HSB again.

3.1. Characteristics of Waves Within and Outside the HSB

The spectra in Plate 1 show that wave activity observed within the HSB has a pattern distinct from that outside the region. Within the HSB, where Ulysses frequently encountered solar wind turbulence, alternating high- and slow-speed solar wind streams, and interplanetary shocks, enhanced and highly variable electric field wave events were observed. The peak power of these waves is seen in a wide range of frequencies from near the local f_{ce} (the white curves overplotted in each panel) to the lowest frequency (0.2 Hz). We will show later that electrostatic waves and electromagnetic waves have been observed in the HSB under different solar wind conditions. At high latitudes outside the HSB, where the solar wind has a relatively constant speed of ~700-800 km/s [*Phillips et al.*, 1995], and the magnitude of the solar wind magnetic field becomes relatively stable as indicated by f_{ce} lines [see also *Balogh et al.*, 1995b], the wave spectra become less variable. Nearly continuous wave activity with relative power peaked near the local f_{ce} was observed. The two distinct patterns of wave spectra within the HSB and in the fast solar wind are consistently observed throughout the mission [see also *Stone et al.*, 1995].

There is an apparent cutoff of wave power at the lowest frequency (9.3 Hz) of the high band, most clearly seen in the spectra of the waves in high-latitude fast solar wind, which is obviously not physical. The apparent cutoff is due to high background noise of the low band, which makes it difficult to detect weaker wave activity. After the background is subtracted from the data, weak signals in the low band may not be seen, while the signals in the high band, which has greater sensitivity, can still be seen. In spite of these background effects, comparison of the spectra in the fast solar wind with the spectra in the HSB, where signals in the high band sometimes disappeared and strong signals in the low band are frequently observed, leads us to believe that the high-latitude fast solar wind conditions are favorable for low-frequency waves to occur. The relative power of these waves observed by Ulysses peaks near the local f_{ce}. The electric component of these waves may extend to lower frequencies but may be too weak to be seen in the low-band channels.

In Figure 3a we show as examples three spectra for periods when Ulysses was in the fast solar wind. Two of them are taken on day 258 of 1994 and day 213 of 1995, when the spacecraft was at the highest southern and northern latitudes (both at $\sim 80.2°$) and at about the same distance from the Sun (~2.28 and 2.02 AU). The third spectrum was taken on day 203 of 1996 ($\sim +31.1°$, 4.11 AU), before the spacecraft reentered the HSB from the north. Each spectrum shows a peak power below but near local f_{ce} (marked with dotted vertical lines in the upper panels), as seen in the plots of the relative intensity (upper panels). The wave power measured at the two polar regions is about the same and has no obvious asymmetry. The wave intensity in the third spectrum is much lower than the other two, mainly due to the much larger distance from the Sun, as the intensity of the waves decreases gradually with increasing distance from the Sun [*Beinroth and Neubauer*, 1981; *MacDowall et al.*, 1996]. In calculating the electric wave power, we have used 23 m as the effective length of the antenna. Note that in each spectrum, there is a smaller peak in the relative intensity near the lowest frequencies. It is produced by large rapid fluctuations of the instrument noise in the channels of 0.3 and 0.4 Hz, and thus there is always noise power detected above the background level determined by our method. This effect caused the nearly continuous enhancements at ~0.3-0.4 Hz seen most of the time in Plate 1.

Magnetic field noise detected by the spin-plane search coil (not shown) in the fast solar wind outside the HSB was near the background level for most of the times. Only when Ulysses approaches within ~1.5-2 AU of the Sun (at the end of 1994 and in 1995 before Ulysses entered and after it exited from the HSB) were magnetic field signals significantly above the background [*Lengyel-Frey et al.*, 1996; *MacDowall et al.*, 1996]. The continuous wave activity in the high-latitude fast solar wind, which was obvious in the electric field data, is not observed in the magnetic field data. This may be because beyond about 2 AU, the intensity of the magnetic component of the waves was usually lower than the instrument background noise.

3.2. Electrostatic and Electromagnetic Waves in the HSB

It is found that the highly variable VLF waves in the HSB consist of electrostatic and electromagnetic waves which occur under different solar wind conditions. Plate 2 shows the data taken within the HSB flows during the fast latitude scan of Ulysses in 1995. The top and

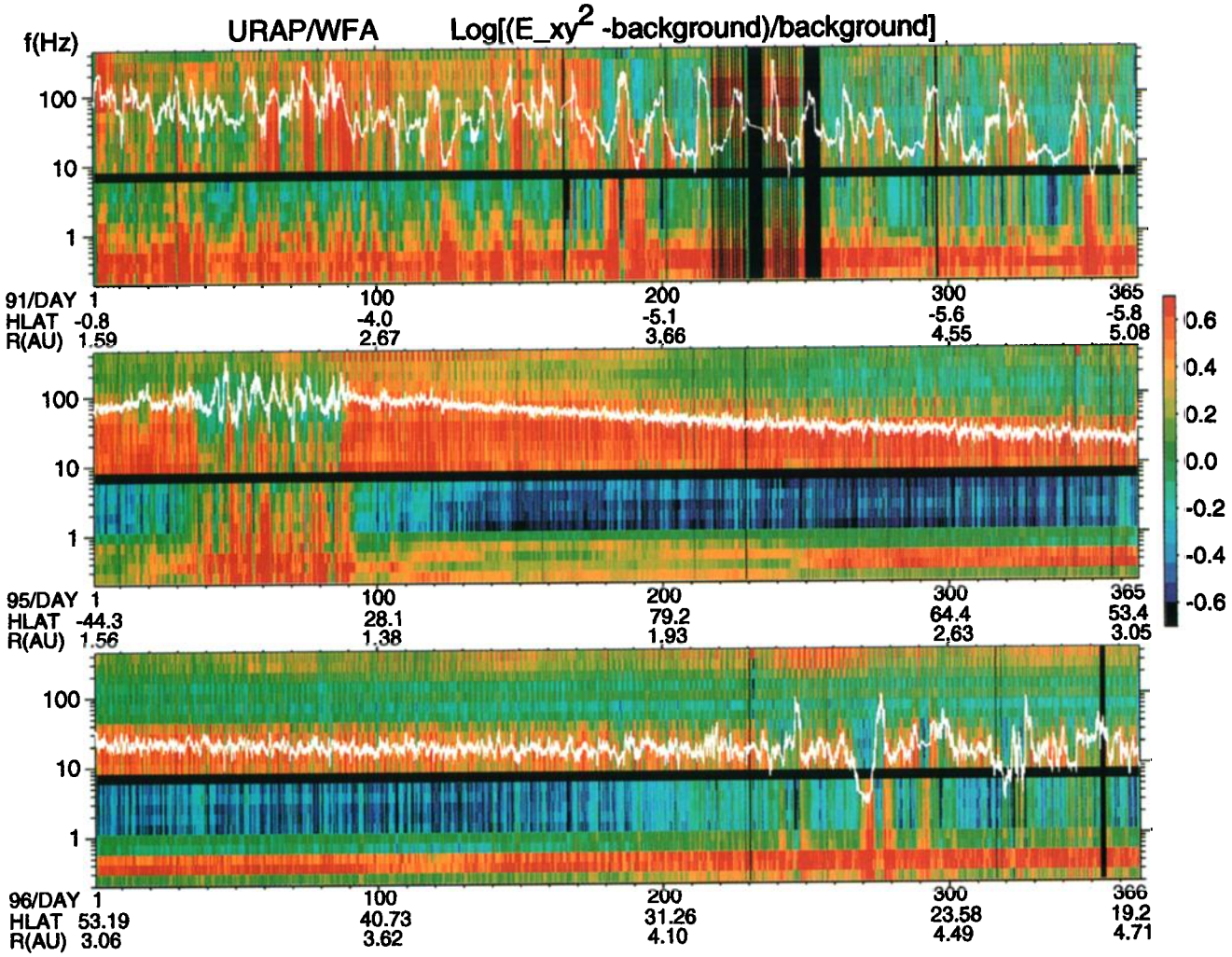

Plate 1. Dynamic spectra of 1-hour averaged relative intensity of spin plane electric wave power for (top) 1991, (middle) 1995, and (bottom) 1996. The horizontal black bar in the middle of each panel is a frequency gap between low-band (0.2-5.3 Hz) and high-band (9.3-448 Hz) channels of the instrument. The vertical black bars crossing all channels are data gaps. The local electron cyclotron frequency is overplotted as a white line in each panel. Day of year, heliographic latitude (HLAT), and distance from the Sun (R, in astronomical units) are indicated. The data of intensity stronger (weaker) than the maximum (minimum) values shown in the color scale to the right are expressed as the color of the maximum (minimum). The enhanced signals in channels of 0.3 and 0.4 Hz, which are seen most of the time, are not real.

bottom panels show the electric field and magnetic field spectra for days 40-70 in the same format as that of Plate 1, but the WFA data are 15-min averages. In the second panel from the top the solar wind velocity for the same period is plotted. The first two vertical dashed lines (on days 41 and 47) mark two forward shocks, and the third line (on day 48) marks a reverse shock. The last three dashed lines mark heliospheric current sheet crossings by Ulysses.

A remarkable feature in the spectra is that strong magnetic wave bursts are observed in the following solar wind conditions: (1) near interplanetary shocks, for example, on days 47 and 48 (we note that there is little wave signature for the shock at the end of day 41, which is a rare exception. Only a few among a few hundred events which are identified as interplanetary shocks have little wave signatures); (2) in the periods of increasing solar wind velocity, for example, on days 43, middle 46-47, 56-59, and 63-64, and day 67; and (3) when the solar wind is more turbulent, which is seen as enhanced fluctuations in the solar wind data, for example, on days 53, 59, and 67. In periods of the first two cases, the ambient magnetic field usually increases, as seen from the f_{ce} lines (white curves in the high-band part of the spectra), and thus the frequency of the waves, which is always below the f_{ce}, extends to higher channels. The magnetic wave bursts in the above three cases are broadband in frequency, extending from a few tens of hertz to the lowest limit of the WFA. The electric component of these waves is observed to be stronger in the high band than in the low band, which indicates that the peak power of these electromagnetic waves may be at about 10-30 Hz, which is a fraction of the local f_{ce} (approximately a few hundreds of hertz). As an

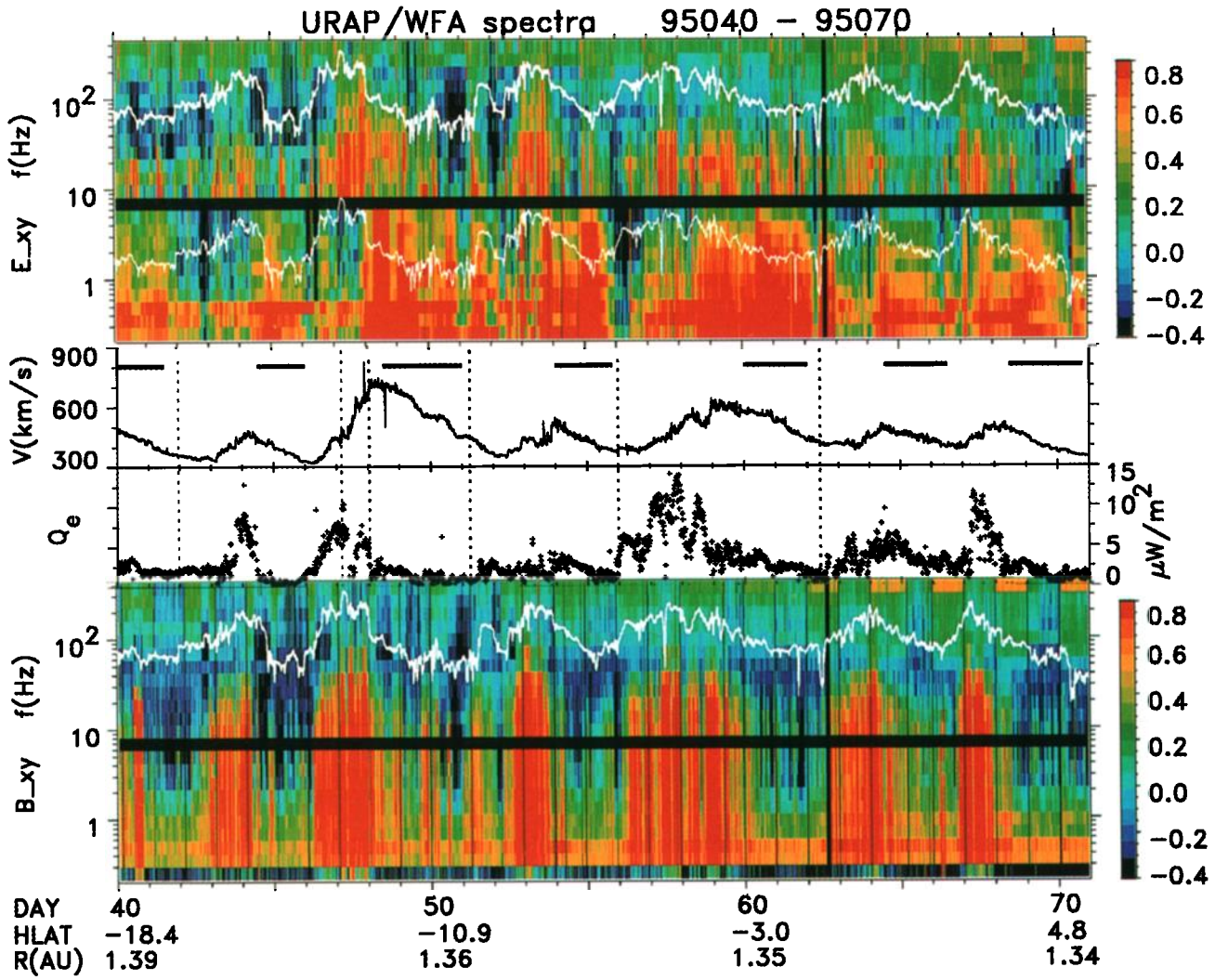

Plate 2. (top to bottom) Spectra of 15-min averaged relative intensity of spin plane electric wave power for the period from day 40 to day 70 of 1995, plotted in the same format as that of Plate 1 (overplotted in the panel with white curves are a local f_{ce} line, which falls in the high band, and a lower hybrid frequency line in the low band); the solar wind velocity in km/s; the electron heat flux in μW/m^2; and magnetic wave power in the same format as that of the electric spectra. The vertical dotted lines mark shock and heliospheric current sheet crossings. The bars in the second panel indicate the periods of decreasing solar velocity.

example of the spectra of these electromagnetic wave bursts, we show in Figure 3b the spectra of electric and magnetic field waves for a 2-hour period on day 47 of 1995. The spectra show that there is significant magnetic wave power (with relative intensity between 1.0 and 2.0) at ~10 Hz and below, while the electric wave power is significant in the high band (above 10 Hz) only. The ratio of CB/E suggests that the waves are likely to be whistler mode. Taking the E and B values at 14 Hz from Figure 3b, we have $CB/E \approx 300$. The index of refraction for whistler mode $n = [f_p^2/f(f_{ce}\cos\theta - f)]^{1/2}$ can be estimated as ~470, which agrees with the CB/E ratio. Here we have taken the wave frequency $f = 14$, the wave angle $\theta = 0°$, the plasma frequency f_p and f_{ce} calculated taking the electron density as about 7/cc (from SWOOPS data), and the magnetic field strength at about 7 nT.

Another remarkable feature in the spectra in Plate 2 is the occurrence of enhanced electric wave bursts during the periods of decreasing solar wind velocity, implying expanding solar wind streams. These periods are marked approximately by bars on the top of the second panel. These waves are apparently electrostatic since there is little corresponding magnetic wave activity observed during these periods. In the spectra of magnetic field waves (the bottom panel) the relative intensity decreases dramatically during these periods. Figure 3c show spectra of these electric waves observed in a 2-hour period on day 55 of 1995. Compared with the spectra in Figure 3b, the electric field spectrum in this example shows a significant wave power at a few hertz (with relative intensity above 0.5), while the magnetic noise is near the background level. During these periods the ambient magnetic field was usually decreasing. (We note that in Plate 2, from the end of day 49 to the

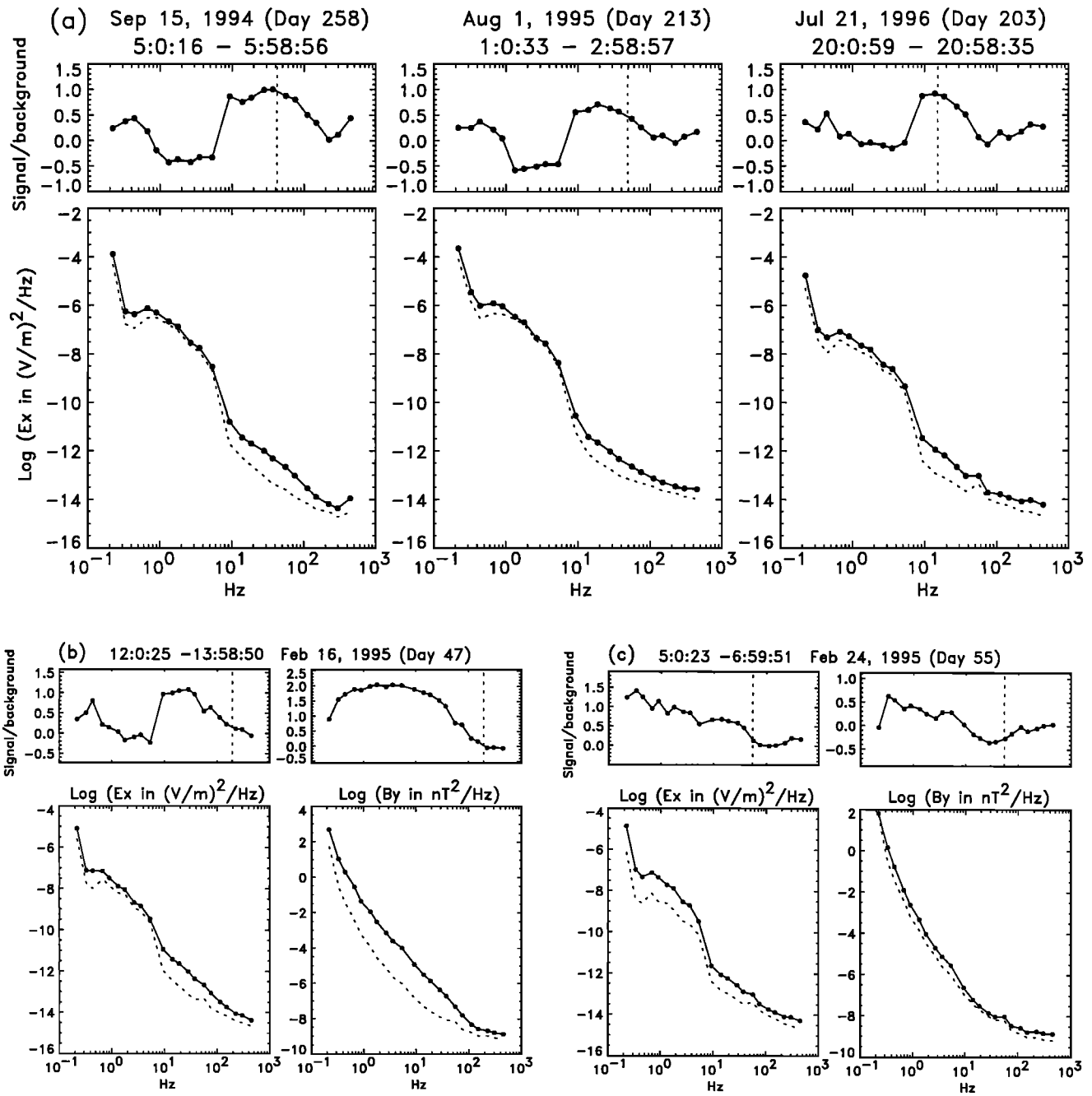

Figure 3. (a) Power spectra of spin plane electric field for three periods in 1994 (heliographic latitude ~−80.2°, at 2.28 AU), 1995 (~+80.2°, 2.02 AU), and 1996 (~+31.1°, 4.11 AU). Plotted in the upper panels is the logarithm of the relative intensity which is used to plot the dynamic spectra in Plate 1. In the lower panels the logarithm of the power density is shown. The instrument background noise is plotted with dotted lines. The solid circles indicate the central frequency of each channel. Vertical dotted lines in the upper panels mark the local f_{ce} for the periods. (b) Power spectra of spin plane (left) electric field and (right) magnetic field for a period between 1200 and 1400 UT, day 47, 1995, plotted in the same format as that of Figure 3a. (c) Power spectra of spin plane (left) electric field and (right) magnetic field for a period between 0500 and 0700 UT, day 55, 1995, plotted in the same format as that of Figure 3c.

beginning of day 50, magnetic wave bursts are observed briefly. This interval occurred as the solar wind velocity became flat and more fluctuating in the middle of the decreasing trend, which again shows that the electromagnetic waves are associated with turbulent solar wind. See also Figure 4.)

The peak power of the electrostatic noise falls mainly in the low band (≤5.3 Hz) and extends to the lowest channel. This frequency range is often near or below the local lower hybrid frequency (the white curve in the low-band spectra), which is calculated as $(f_{ce}f_{ci})^{1/2}$, where f_{ci} is the proton gyrofrequency.

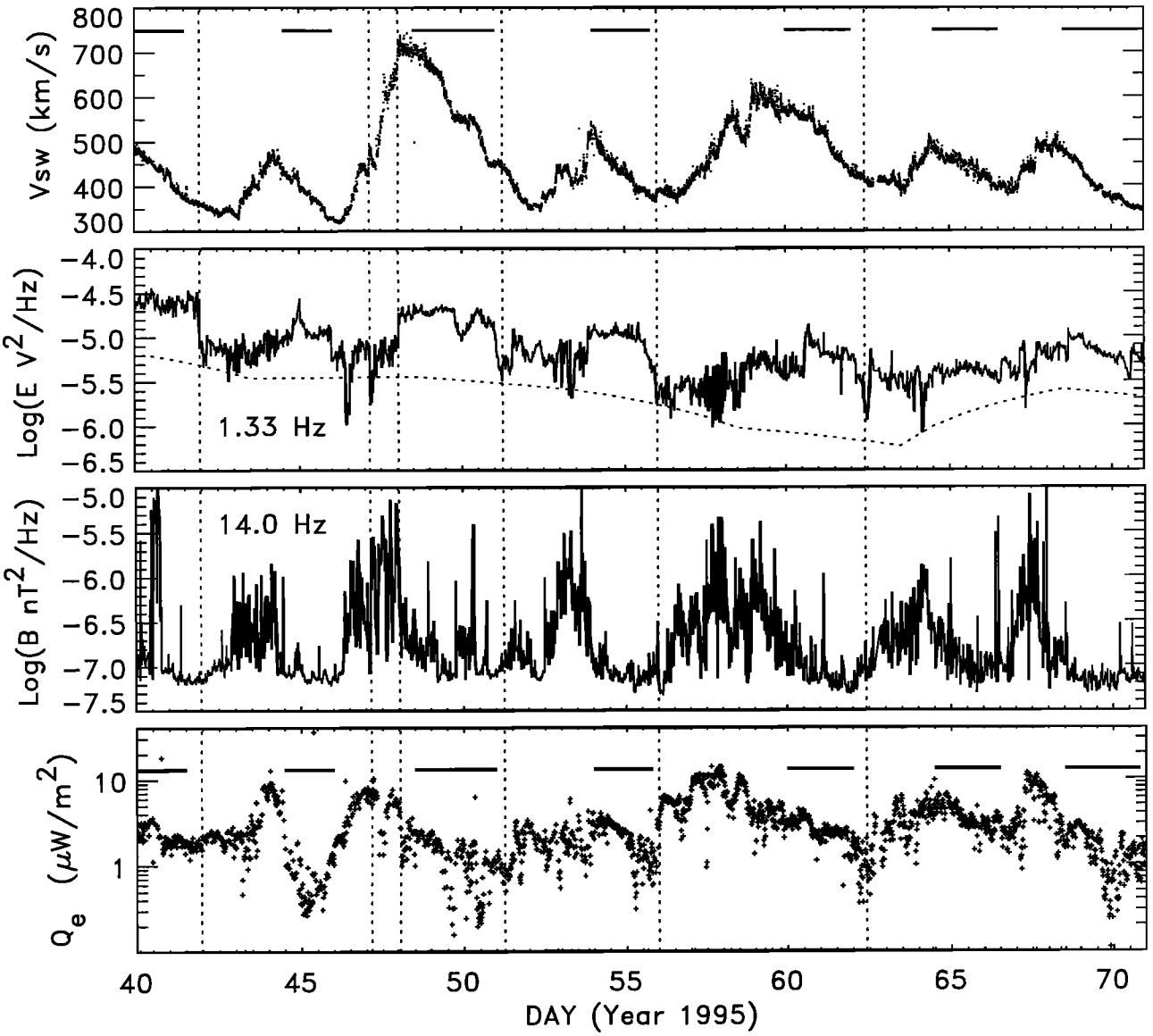

Figure 4. Data for the period from day 40 to 70 of 1995. (top to bottom) The solar wind velocity in km/s; logarithm of spin plane electric wave power density (in V^2/Hz, 15-min averages) for 1.33-Hz channel (the dashed curve is the background level); logarithm of spin plane magnetic wave power density (in nT^2/Hz, 15-min averages) for 14-Hz channel; and the electron heat flux in $\mu W/m^2$ plotted in the log scale. The vertical dotted lines mark shock and heliospheric current sheet crossings. The bars in the top and bottom panels indicate the periods of decreasing solar wind velocity when enhanced electrostatic waves are seen.

3.3. Relation Between the Electron Heat Flux and the VLF Waves

In Plate 2 the electron heat flux Q_e is plotted in the third panel from the top. The heat flux is calculated from equation (2) of *Scime et al.* [1994]:

$$\mathbf{Q_e} = \int \frac{m}{2}\mathbf{U}U^2 f_e d^3v,$$

where $\mathbf{U} = \mathbf{v} - < v >$. It is found, in general, that the heat flux level increased significantly during the periods of increasing solar wind velocity, near interplanetary shocks, and when the solar wind was more turbulent, i.e., during the periods when we observed enhanced electromagnetic waves, while in the expanding solar wind, when enhanced electrostatic noise was observed, the heat flux decreased to and remained at a lower level.

These correlations between the wave intensity, the solar wind velocity, and the heat flux can be better observed in Figure 4, which shows line plots of the data in Plate 2. The electric field waves are represented by a channel with central frequency at 1.33 Hz (second panel), and the magnetic field waves are represented by a channel of 14.0 Hz (third panel). The figure shows that strong magnetic wave bursts are mainly associated

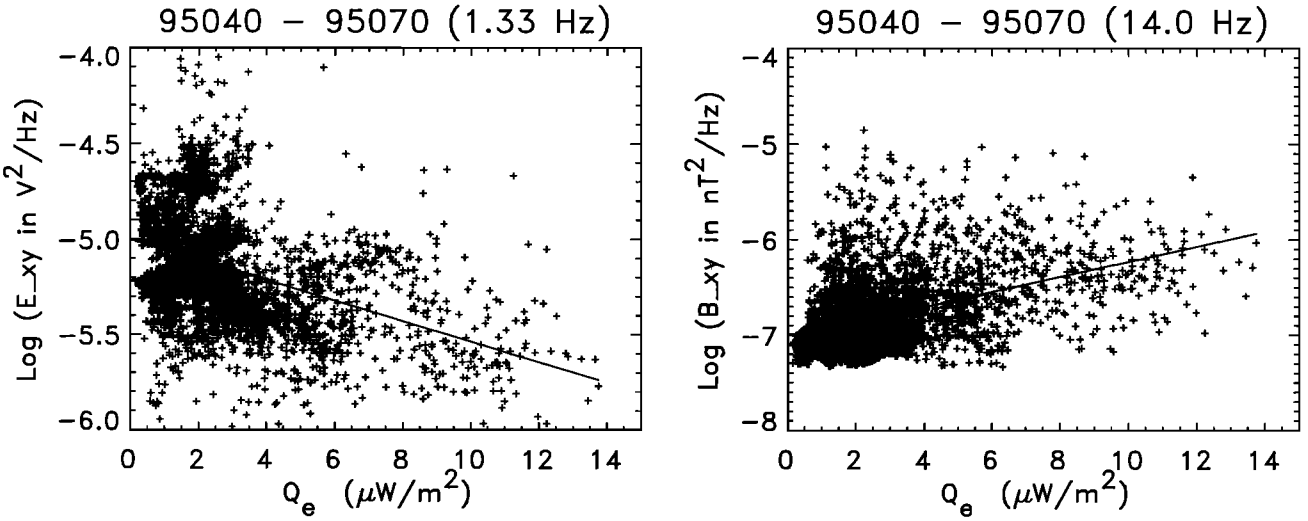

Figure 5. The logarithm of the spin plane (left) electric wave power at 1.3 Hz and (right) magnetic wave power at 14 Hz versus the electron heat flux, for days 40-70 of 1995. The wave data are 15-min averages. The straight lines are the linear fit of the data.

with increasing solar wind velocity and are coincident with the bursts of high-level heat flux (~4 $\mu W/m^2$ and above). In these intervals, the electric field intensity is relatively low, often reduced to near background level (the dashed curve in the second panel). Examples of such intervals can be found between two shocks on days 47 and 48, and between days 56 and 58. In contrast, in the intervals of decreasing solar wind velocity (the intervals marked with the bars) the electric field increased to a level well above the background, while the magnetic wave intensity dropped to near background. Note that the magnetic signals at lower frequencies have the same variation as that for the channel shown (see Plate 2). In these intervals, the electron heat flux was usually low (~1-2 $\mu W/m^2$ or lower). In Figure 5 we show this relation between electric and magnetic waves and the heat flux level by plotting the logarithm of the wave power versus heat flux, Q_e. The left panel shows that the high-intensity E field is associated with low Q_e (below ~3 $\mu W/m^2$), while at high Q_e, the E field power is low. The magnetic wave power (right panel) varies in the opposite way, with the wave power tending to increase with increasing Q_e. The linear fit lines overplotted are to show the trend of the relationship only.

The above occurrence pattern of VLF waves under different solar wind conditions has been frequently observed throughout the mission [see also *Lin et al.*, 1997], from the ecliptic plane to medium heliospheric latitudes as long as Ulysses was in the HSB. In Figure 6 we show similar observations for the first 120 days of 1993, before the heliospheric current sheet ceased to be seen by Ulysses at heliographic latitudes ~−30° [*Smith et al.*, 1993]. During this period the spacecraft was in the midheliographic latitudes of ~−22.7° to ~−29.7° at a distance of ~5.06-4.77 AU from the Sun. The recurrent high-speed (~700-800 km/s) solar wind streams are obvious in the top panel. The source of the major recurrent high-speed streams is believed to be the equatorward extension of the polar coronal hole, while the valleys between stream peaks are due to crossings of the heliomagnetic streamer belt [*Bame et al.*, 1993]. Unlike the period shown in Figure 4, the increases of the solar wind speed in Figure 6 are often very steep and are accompanied by shock crossings (marked with vertical dotted lines). As a result, significant magnetic wave bursts are observed only in short intervals near interplanetary shocks (see the third panel). Similar to the case in the 1995 period (Figure 4), the strong magnetic wave bursts are coincident with significant reductions in intensity of the electric field at lower frequencies (represented by the 0.89-Hz channel in the second panel) and large increases in the electron heat flux. The occurrences of these short intervals are marked approximately with solid circles in the second panel. Note that the overall heat flux level is about 10 times lower than that in the 1995 period, because the spacecraft was at a farther distance from the Sun in this period, and the electron heat flux decreases rapidly with heliocentric distance [*Scime et al.*, 1994].

In the rarefaction regions, in which the solar wind velocity was decreasing (marked with the solid bars in the top and bottom panels), the magnetic search coil of the WFA recorded mainly the background noise. Magnetometer data [*Smith et al.*, 1993] also show that these intervals are intervals of unusually low and quiet magnetic field, but in these intervals, we observed enhanced electric waves, which are well above the background. As in the case of the 1995 period, the frequency of these waves extends to the lowest channel of the instrument. The heat flux levels in these intervals are usually very low, usually less than ~0.2 $\mu W/m^2$. We note that in some cases when the spacecraft was not close to any shock, we observed a significant increase in electron heat flux when the intensity of electric waves decreased. Two of such examples are marked with open circles in the second panel of Figure 6.

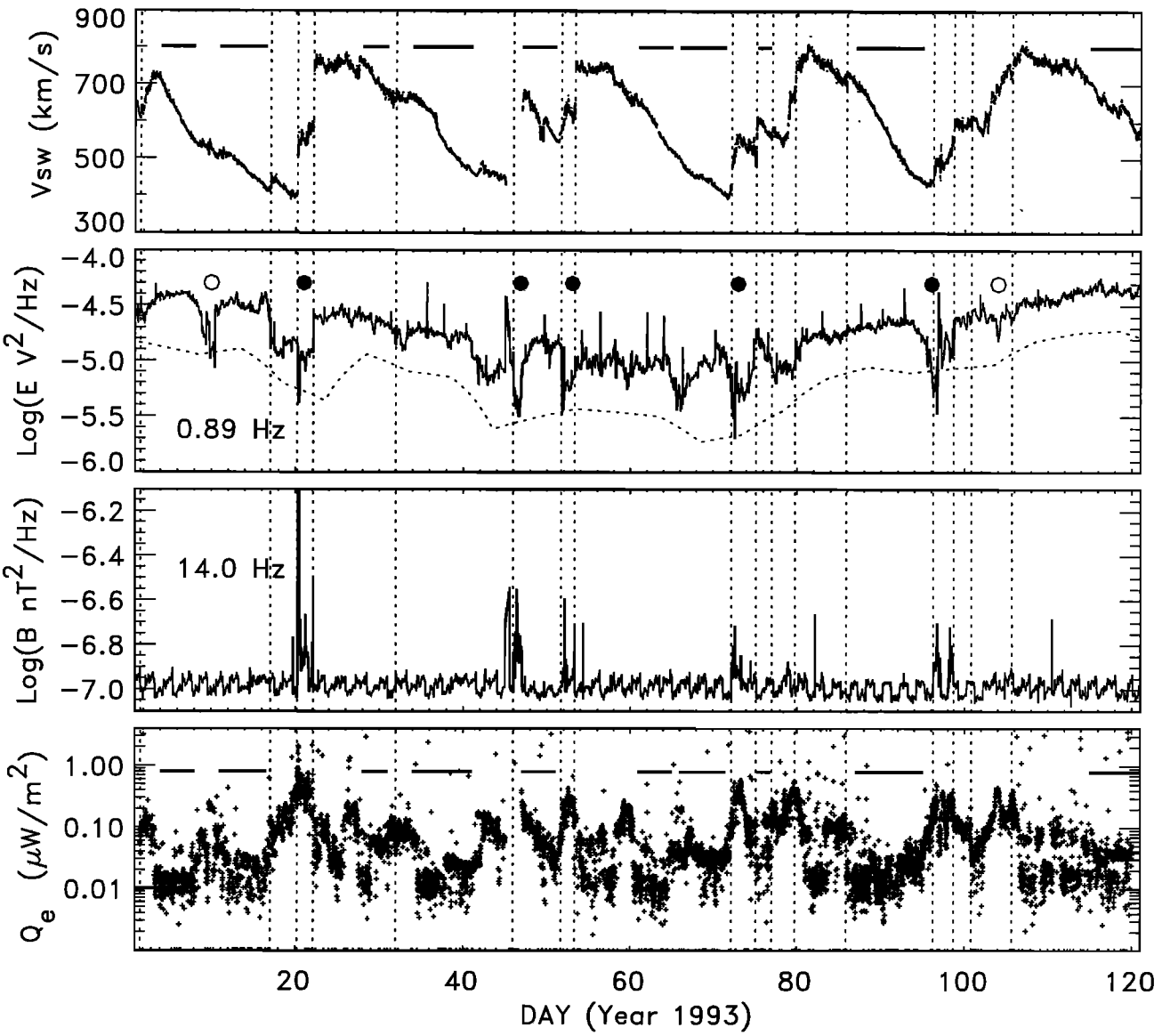

Figure 6. Similar to Figure 4 but for the first 120 days in 1993. The electric wave data are for the 0.89-Hz channel. Both electric and magnetic wave data are 1-hour averages. All vertical lines indicate shock crossings. The solid and open circles in the second panel indicate brief periods of reduced electric wave power.

3.4. Summary of the Observations

We have presented the overall profile of wave activity in the heliosphere through Ulysses observations in a ~6-year period. It has been seen that the interplanetary medium, especially in the HSB, is rich with wave activity in a frequency range below and near the local electron cyclotron frequency.

Intense electromagnetic waves have been observed in turbulent solar wind, near shocks, and in periods of increasing solar wind velocity. The magnetic component of these waves has a broad frequency range (from a few tens of hertz to the lowest frequency of our instrument) (see Figure 3b), but the spectra of relative intensity of the electric component seem to show that the peak power of these waves is at about 10-20 Hz, which is a fraction of the local f_{ce}. The occurrences of these electromagnetic waves are usually coincident with a large increase in the electron heat flux.

In the periods of expanding solar wind, i.e., where the spacecraft observed decreasing solar wind speed, enhanced electric field waves are observed. These wave are apparently electrostatic, since little significant magnetic component is observed (Figure 3c). During these periods, the electron heat flux usually decreased remarkably, to a level a few times to more than 10 times lower than its highest levels, which were often seen in the vicinity of an interplanetary shock or in the periods of increasing solar wind speed, prior to to the expanding solar wind periods.

The above electromagnetic and electrostatic waves are observed in the HSB region. Outside the region are fast solar wind streams (~700-800 km/s), which em-

anated from the south or north polar coronal holes. In such fast solar wind, VLF waves occur almost continuously with the observed relative power peaked near f_{ce} (a few tens of hertz). They are less variable in frequency range and in intensity, but the intensity gradually decreases with increasing distance from the Sun, and the frequency of the peak power also decreases as the f_{ce} decreases with the increasing distance.

4. Discussion

Magnetic field waves observed by Ulysses in the vicinity of interplanetary shocks and in the turbulent solar wind as presented here are similar in nature to those reported in the previous missions reviewed in the introduction section. Their frequencies fall within the whistler mode frequency range. The example event in Figure 3b shows that the B/E ratio of the waves is consistent with the dispersion relation of the whistler mode waves. Studying Ulysses URAP wave data, *Lengyel-Frey et al.* [1996] have shown that whistler waves are observed downstream of almost all Ulysses shocks and are observed upstream when the spacecraft is within a heliocentric distance of about 2 AU. The waves observed downstream of a shock may last for many hours. *Lengyel-Frey et al.* [1994] have also found that in the several interplanetary shocks they studied, the whistler waves observed downstream of the shocks were highly oblique, with propagation angles ranging from ~50° to 70°.

From Plate 2 and Figure 4, it is obvious that strong magnetic wave bursts also occur in regions of increasing solar wind velocity, not necessarily in the vicinity of a shock. These regions are often compression regions of high-speed stream interfaces. This is similar to what has been observed by Helios at 0.3-1 AU from the Sun [*Beinroth and Neubauer*, 1981]. *Eviatar and Goldstein* [1980] discussed theoretically several plasma instabilities which were associated with stream interfaces and the compression region. They found that beyond 1 AU, the possible range of frequencies excited in these regions extends from the lower hybrid (due to the modified two-stream instability) through the ion acoustic frequency range to harmonics of the electron cyclotron frequency. More detailed studies are needed to compare these theoretical predictions with the observed data. Because the Ulysses trajectory covers much larger distances from the Sun and higher latitudes than the Helios orbit, the spacecraft has spent much more time in the rarefaction regions. The fact that the magnetic wave power decreases to near or below instrument noise level, in contrast to the strong bursts in the leading edges of fast stream events, as clearly seen in Figures 4 and 6, suggests that the plasma conditions in the rarefaction regions do not favor the excitation of electromagnetic whistler mode waves.

A combination of various energy sources may contribute to the excitation of the whistler waves in turbulence solar wind, especially near interplanetary shocks. *Pierre et al.* [1995] reported that there was evidence in Ulysses observations that the electron temperature anisotropy [*Kennel*, 1966] was a possible free-energy source for the wave growth near interplanetary shocks. The coincidence between the enhancement of the magnetic waves and the large increase in the electron heat flux suggests that the whistler heat flux instability [e.g., *Gary et al.*, 1975a, b; *Gary et al.*, 1994] may also play an important role in the excitation of the magnetic waves.

While the magnetic field waves basically vanish during the rarefaction periods, electric field noise enhances significantly at frequencies of a few hertz to a fraction of a hertz. To our knowledge, the occurrence of enhanced electrostatic noise in periods of decreasing solar wind speed has not been reported before. It is very interesting to find that the enhancements of these low-frequency electric waves are coincident with significant reductions of the electron heat flux. This may imply that these waves are associated with the electron heat flux regulation in the solar wind.

It has long been suggested that to account for the electron heat flux regulation in the solar wind, heat flux limiting instabilities should be considered [e.g., *Feldman*, 1979; *Gary and Feldman*, 1977]. Among those instabilities, the whistler mode is likely to generate wave activity in the frequency range that we observed. For example, the frequencies at which the whistler heat flux instability grows are near 100 f_{ci} [*Gary et al.*, 1975a]. In the rarefaction periods in Figure 4 when the heat flux level was low, the proton gyrofrequency is $f_{ci} \approx 0.02 - 0.03$ Hz. Thus the waves observed should fall in the low-band channel, which is what we see. *Gary et al.* [1994] have examined the threshold of the heat flux instability with a global model based on average electron properties observed during the in-ecliptic phase (1-5 AU) of the Ulysses mission [*Scime et al.*, 1994] and found that the upper bound and radial scaling for the electron heat flux predicted by the theoretical model are consistent with the observations [see *Scime et al.*, 1994, Figure 11e]. By changing $T_{\parallel}/T_{\perp}$ of halo electrons from 0.735 used by *Gary et al.* [1994] to 0.95, *Scime et al.* [1994] obtained the heat flux magnitude and radial scaling which match the observations better. We note that the calculated heat flux, which is assumed to be regulated by the instability, is ~0.1 $\mu W/m^2$ between 4.5 and 5 AU and is ~3-4 $\mu W/m^2$ near 1.35 AU. These numbers agree with the low heat flux levels in the expanding solar wind periods in our Figure 6 (~4.5-5 AU) and Figure 4 (~1.34-1.4 AU). This implies that the heat flux level during these expanding solar wind periods may be marginally sufficient to drive the whistler heat flux instability.

We note that the whistler heat flux instability [*Gary et al.*, 1994] has maximum growth rate in the direction parallel to the background magnetic field and produces primarily magnetic fluctuations. If this instability would reduce the heat flux level, we would expect to see magnetic waves also in the periods of low heat flux level. This contradicts what we see. The observations show that low heat flux is coincident with electric field waves and limited magnetic fluctuations. One possibility is that the waves propagate obliquely near the resonance cone and so have a large E/B ratio and are observed to

be primarily electrostatic. Also, most plasma instabilities are sensitive to the precise shape of the distribution function. The above theory of the whistler instability is based on the assumption of bi-Maxwellian core and halo electron distributions. In future work, to understand the mechanism of these electric waves, we may need to modify the existing theory by looking into the distributions of electrons in more detail and determining the propagation angle of the waves.

Marsch and Chang [1982] have suggested that in a typical solar wind plasma, "hybrid" whistler modes can be excited with the free energy provided by resonant halo electrons. These waves propagate at large oblique angles and become nearly electrostatic. The cutoff frequency of these electrostatic modes is near the lower hybrid frequency. From the electric field spectra displayed in Plate 2, the enhanced electric waves extend well below the local lower hybrid frequency, which does not seem to agree with the mechanism.

The waves occurring in the fast solar wind outside the HSB may be electromagnetic waves. Although the instrument did not detect significant magnetic noise beyond about 2 AU, we still observed almost continuous magnetic noise from about 10 to 20 Hz and below, when the spacecraft was closer to the Sun but was in the high-latitude fast solar wind [see, for example, *Lengyel-Frey et al.*, 1996, Figures 7 and 8]. The frequency range of the waves suggests that these waves may also be whistler mode. The heat flux level in high-latitude fast solar wind is less variable and also less dissipated [*Scime et al.*, 1995]. It is not yet clear if the heat flux instability also plays a role in the excitations of the observed high-latitude waves.

Acknowledgments. The URAP experiment is a collaboration of NASA Goddard Space Flight Center, the Observatoire de Paris-Meudon, the University of Minnesota, and the Centre des Etudes Terrestres et Planetaires, Velizy, France. The work at Los Alamos was carried out under the auspices of the U.S. Department of Energy with support from NASA. Author N.L. thanks S. P. Gary for many helpful discussions. He also thanks K. Goetz and S. J. Monson of the University of Minnesota for data interpretation and support in conducting this study.

The Editor thanks Donald B. Melrose and Steven J. Schwartz for their assistance in evaluating this paper.

References

Balogh, A., T. J. Beek, R. J. Forsyth, P. C. Hedgecock, R. J. Marquedant, E. J. Smith, D. J. Southwood, and B. T. Tsurutani, The magnetic field investigation on the Ulysses mission: Instrumentation and preliminary scientific results, *Astron. Astrophys. Suppl. Ser., 92*, 221, 1992.

Balogh, A., J.-A. Gonzalez-Esparza, R. J. Forsyth, M. E. Burton, B. E. Goldstein, E. J. Smith, and S. J. Bame, Interplanetary shock waves: Ulysses observations in and out of the ecliptic plane, *Space Sci. Rev., 72*, 171, 1995a.

Balogh, A., E. J. Smith, B. T. Tsurutani, D. J. Southwood, R .J. Forsyth, and T. S. Horbury, The heliospheric magnetic field over the south polar region of the sun, *Science, 268*, 1007, 1995b.

Bame, S. J., D. J. McComas, B. L. Barraclough, J. L. Phillips, K. J. Sofaly, J. C. Chavez, B. E. Goldstein, and R. K. Sakurai, The Ulysses solar wind plasma experiment, *Astron. Astrophys. Suppl. Ser., 92*, 237, 1992.

Bame, S.J., B.E. Goldstein, J.T. Gosling, J.W. Harvey, D.J. McComas, M. Neugebauer, and J.L. Phillips, Ulysses observations of a recurrent high-speed solar wind stream and the heliomagnetic streamer belt, *Geophys. Res. Lett., 20*, 2323, 1993.

Beinroth, H. J., and F. M. Neubauer, Properties of whistler mode waves between 0.3 and 1.0 AU from Helios, *J. Geophys. Res., 86*, 7755, 1981.

Coles, W. A., Interplanetary scintillation observations of the high-latitude solar wind, *Space Sci. Rev., 72*, 171, 1995.

Coroniti, F. V., C. F. Kennel, F. L. Scarf, and E. J. Smith, Whistler mode turbulence in the disturbed solar wind, *J. Geophys. Res., 87*, 6029, 1982.

Eviatar, A., and M. L. Goldstein, Microscale instabilities in stream interaction regions, *J. Geophys. Res., 85*, 753, 1980.

Feldman, W. C., Kinetic processes in the solar wind, in *Solar System Plasma Physics*, edited by C. F. Kennel, L. J. Lanzerotti, and E. N. Parker, Vol I, pp. 321-344, North-Holland, New York, 1979.

Forsyth, R.J., A. Balogh, T. S. Horbury, G. Erdvs, E. J. Smith, and M. E. Burton, The heliospheric magnetic field at solar minimum: Ulysses observations from pole to pole, *Astron. Astrophys., 316*, 287, 1996.

Gary, S. P., and W. C. Feldman, Solar wind heat flux regulation by the whistler instability, *J. Geophys. Res., 82*, 1087, 1977.

Gary, S. P., W. C. Feldman, D. W. Forslund, and M. D. Montgomery, Electron heat flux instabilities in the solar wind, *Geophys. Res. Lett., 2*, 79, 1975a.

Gary, S. P., W. C. Feldman, D. W. Forslund, and M. D. Montgomery, Heat flux instabilities in the solar wind, *J. Geophys. Res., 80*, 4197, 1975b.

Gary, S. P., E. E. Scime, J. L. Phillips, and W. C. Feldman, The whistler heat flux instability: Threshold conditions in the solar wind, *J. Geophys. Res., 99*, 23,391, 1994.

Gurnett, D. A., Waves and instabilities, in *Physics of the Inner Heliosphere*, edited by. R. Schwenn and E. Marsch, pp. 135-157, Springer-Verlag, New York, 1991.

Gurnett, D. A., F. M. Neubauer, and R. Schwenn, Plasma wave turbulence associated with interplanetary shocks, *J. Geophys. Res., 84*, 541, 1979a.

Gurnett, D. A., E. Marsch, W. Pilipp, R. Schwenn, and H. Rosenbauer, Ion acoustic waves and related plasma observations in the solar wind, *J. Geophys. Res., 84*, 2029, 1979b.

Kellogg, P. J., K. Goetz, N. Lin, S. J. Monson, A. Balogh, R. J. Forsyth, and R. G. Stone, Low frequency magnetic signals associated with Langmuir waves, *Geophys. Res. Lett., 19*, 1299, 1992.

Kennel, C. F., Low frequency whistler mode, *Phys. Fluids, 9*, 2190, 1966.

Kennel C. F., F. L. Scarf, F. V. Coroniti, E. J. Smith and D. A. Gurnett, Nonlocal plasma turbulence associated with interplanetary shocks, *J. Geophys. Res., 87*, 17, 1982.

Lengyel-Frey, D., W.M. Farrell, R.G. Stone, A. Balogh, and R. Forsyth, An analysis of whistler waves at interplanetary shocks, *J. Geophys. Res., 99*, 13,325, 1994.

Lengyel-Frey, D., R. Hess, R.J. MacDowall, R.G. Stone, N. Lin, A. Balogh, and R. Forsyth, Ulysses observations of whistler waves at interplanetary shocks and in the solar wind, *J. Geophys. Res., 101*, 27,555, 1996.

Lin, N., P. J. Kellogg, R. J. MacDowall, E. E. Scime, J. L. Phillips, A. Balogh, and R. J. Forsyth, Low frequency plasma waves in the solar wind: from ecliptic plane to the

solar polar regions, *Adv. Space. Res., 19(6)*, pp. 877-881, 1997.

MacDowall, R.J., R.A. Hess, N. Lin, G. Thejappa, A. Balogh, and J.L. Phillips, Ulysses spacecraft observations of radio and plasma waves: 1991-1995, *Astron. Astrophys., 316*, 396, 1996.

Marsch, E., and T. Chang, Lower hybrid waves in the solar wind, *Geophys. Res. Lett., 9*, 1155, 1982.

Marsch, E., and T. Chang, Electromagnetic lower hybrid waves in the solar wind, *J. Geophys. Res., 88*, 6869, 1983.

Neubauer, F. M., H. J. Beinroth, H. Barnstorf, and G. Dehmel, Initial results from the Helios-1 Search-Coil magnetometer experiment, *J. Geophys., 42*, 599, 1977a.

Neubauer, F. M., G. Musmann, and G. Dehmel, Fast magnetic fluctuations in the solar wind: Helios 1, *J. Geophys. Res., 82*, 3201, 1977b.

Phillips, J.L., et al., Ulysses solar wind plasma observations at high southerly latitudes, *Science, 268*, 1030, 1995.

Pierre, F., J. Solomon, N. Cornilleau-Wehrlin, P. Canu, E.E. Scime, J. Phillips, A. Balogh, and R. Forsyth, Whistler-mode wave generation around interplanetary shocks in and out of the ecliptic plane, *Geophys. Res. Lett., 22*, 3425, 1995.

Scarf, F. L., J. H. Wolfe, and R. W. Silva, A plasma instability associated with thermal anisotropies in the solar wind, *J. Geophys. Res., 72*, 993, 1967.

Schwartz, S. J., Plasma instabilities in the solar wind: A theoretical review, *Rev. Geophys., 18*, 313, 1980.

Scime, E. E., S.J. Bame, W.C. Feldman, S.P. Gary, J.L. Phillips, and A. Balogh, Regulation of the solar wind electron heat flux from 1 to 5 AU: Ulysses observations, *J. Geophys. Res., 99*, 23,401, 1994.

Scime, E. E., S.J. Bame, J.L. Phillips, and A. Balogh, Latitudinal variations in the solar wind electron heat flux, *Space Sci. Rev. 72*, 105, 1995.

Smith, E.J., M. Neugebauer, A. Balogh, S. J. Bame, G. Erdvs, R. J. Forsyth, B. E. Goldstein, J. L. Phillips, and B. T. Tsurutani, Disappearance of the heliospheric sector structure at Ulysses, *Geophys. Res. Lett., 20*, 2327, 1993.

Stone, R. G., et al., The unified radio and plasma wave investigation, *Astron. Astrophys. Suppl. Ser., 92*, 291, 1992.

Stone, R. G., et al., Ulysses radio and plasma wave observations from the ecliptic to high southern heliographic latitudes, *Science, 268*, 1026, 1995.

A. Balogh and R. J. Forsyth, Imperial College of Science and Technology, London, England. (e-mail: a.balogh @ic.ac.uk; r.forsyth@ic.ac.uk)

P. J. Kellogg and N. Lin, School of Physics and Astronomy, University of Minnesota, Minneapolis, MN 55455. (e-mail: lin@waves.space.umn.edu; kellogg@ waves.space.umn.edu)

R. J. MacDowall, NASA Goddard Space Flight Center, Greenbelt, MD 20771. (e-mail: xrrjm@leprjm.gsfc.nasa. gov)

D. J. McComas and J. L. Phillips, Los Alamos National Laboratory, Los Alamos, NM 87545. (e-mail: dmccomas@lanl.gov)

E. E. Scime, Physics Department, West Virginia University, Morgantown, WV 26506. (e-mail: scime@ wvnvaxa.wvnet.edu)

(Received September 26, 1997; revised December 16, 1997; accepted March 4, 1998.)